Root architecture and wind-firmness of mature *Pinus pinaster*

Frédéric Danjon[1], Thierry Fourcaud[2,3] and Didier Bert[1]

[1]INRA – Bordeaux, EPHYSE – 69, route d'Arcachon, F–33612 Gazinet Cedex, France; [2]CIRAD Departement AMIS – Laboratoire de Rhéologie du Bois de Bordeaux (UMR CNRS, INRA, Université Bordeaux I, 69 route d'Arcachon, F–33612 Gazinet Cedex, France; [3]Present address: LIAMA – Institute of Automation, Chinese Academy of Sciences, PB 2728, Beijing 100080, China

Summary

Author for correspondence:
Frédéric Danjon
Tel: +33 (0)5 57122845
Fax: +33 (0)5 56680223
Email: fred@pierroton.inra.fr

• This study aims to link three-dimensional coarse root architecture to tree stability in mature timber trees with an average of 1-m rooting depth.
• Undamaged and uprooted trees were sampled in a stand damaged by a storm. Root architecture was measured by three-dimensional (3-D) digitizing. The distribution of root volume by root type and in wind-oriented sectors was analysed.
• Mature *Pinus pinaster* root systems were organized in a rigid 'cage' composed of a taproot, the zone of rapid taper of horizontal surface roots and numerous sinkers and deep roots, imprisoning a large mass of soil and guyed by long horizontal surface roots. Key compartments for stability exhibited strong selective leeward or windward reinforcement. Uprooted trees showed a lower cage volume, a larger proportion of oblique and intermediate depth horizontal roots and less wind-oriented root reinforcement.
• *Pinus pinaster* stability on moderately deep soils is optimized through a typical rooting pattern and a considerable structural adaptation to the prevailing wind and soil profile.

Key words: biomechanics, forest tree, hard pan, *Pinus pinaster*, structural plasticity, three-dimensional (3-D) coarse root architecture, tree stability, windthrow.

Introduction

During the past 30 yr, many forests of Western Europe have been severely damaged by several major storms (Stokes, 2002), which has increased interest in the mechanisms involved in uprooting. The resistance of forest trees to breakage or overturning in windy climates largely depends on structural modifications to achieve mechanical strength, and the biomass allocation within the root system has a marked effect on tree stability (Nicoll & Ray, 1996). Mechanical stress can play a fundamental role in the development of root structures, causing significant changes to the allocation rules that act to optimize tree stability (Nicoll *et al.*, 1995; Stokes *et al.*, 1997).

The quantitative assessment of tree coarse root architecture was first achieved by measuring cross-sectional areas (CSA) of

the second-order surface roots of *Picea sitchensis* (Bong.) Carr. growing on shallow soils (Coutts, 1983b). In deep root systems, CSA measurements have now been overtaken by recently available three-dimensional (3-D) digitizing methods (Danjon *et al.*, 1999a,b; Oppelt *et al.*, 2000), which had never previously been applied to large root systems. Radar imaging can mainly be used for biomass estimation in specific types of soils and needs to be further developed (Butnor *et al.*, 2001).

A large number of parameters on the location of root quantities can be computed from 3-D digitizing data of whole root systems, including (1) CSAs in any location, (2) bulk root volume distribution as a function of depth, azimuth, radial distances and root inclination, and (3) root volume in the root compartments such as taproot and sinkers. To date, only analyses of type (2) have been employed (Danjon *et al.*, 1999a,b). Type (3) analyses may

provide a better insight into the allocation of resources to corresponding root types in species whose root systems are structured in several distinct root types.

The mechanics of tree anchorage cannot generally be monitored during a storm, but relationships between root architecture and wind-firmness can be studied using the following three types of technique.

(a) Tree pulling tests combined with simple root-soil plate, tree biomass or architecture measurements (e.g. Coutts, 1983b; Crook & Ennos, 1996; Cucchi *et al.*, 2004) permit measurement of the parameters involved in uprooting, but only partially mimic what happens during a storm.

(b) Surveys of storm damage at the stand and tree levels (Mason, 1985; Harrington & DeBell, 1996; Cucchi & Bert, 2003) make it possible to link tree characteristics to wind effects, despite the fact that the parameters determining failure are unknown, and weather and soil conditions will be specific.

(c) The mechanical modelling and simulation of anchorage in real or virtual soil, and data on wind and tree architecture (Blackwell *et al.*, 1990; Fourcaud *et al.*, 2003b; Dupuy *et al.*, 2005b).

The factors affecting tree resistance to uprooting have mainly been studied using technique (a) in *P. sitchensis* with a rooting depth of < 50 cm (Coutts *et al.*, 1999). The radial symmetry of second-order surface roots appeared to determine anchorage strength (Coutts *et al.*, 1999). Irregularities in the soil such as plough furrows, old stumps and microtopography may strongly influence root system morphogenesis (Henderson *et al.*, 1983; Coutts *et al.*, 1990). In response to wind movement, trees develop an oval, I-beam or T-beam shaped diameter reinforcement of shallow horizontal roots, near the stump (Coutts *et al.*, 1999). This region has been termed the 'zone of rapid taper' (Eis, 1974) and is of major importance to anchorage (Coutts, 1987). In deeper-rooted small trees, the tap root plays a predominant role which is supplemented by the sinker roots (Crook & Ennos, 1996). In planted saplings of *P. pinaster*, stem straightness is promoted by rooting depth, a high root-shoot ratio and a high proportion of deep roots. Vertical rooting can be altered by inappropriate planting methods (Danjon *et al.*, 1999a,b). Genetic factors control about one-quarter of stem straightness variability in 10-yr-old stands (Danjon, 1994). Artificial unidirectional wind loading or flexing experiments in tree seedlings have generally resulted in an increase in root size and number along the axis of flexing (Stokes *et al.*, 1997; Tamasi *et al.*, 2005). However, we lack knowledge in many areas of tree stability and root anchorage (Stokes, 2002), particularly in mature timber trees exhibiting moderate rooting depth.

Twenty-five million cubic metres of the intensively managed Landes de Gascogne *P. pinaster* forest in France was damaged by the storms on December 27 and 28, 1999, corresponding to one-fifth of the standing volume (Cucchi & Bert, 2003). This event provided an unique opportunity to link root system architecture to tree stability using technique (b) in mature *P. Pinaster* grown on sandy spodosol where root growth ceased at a depth of 1 m, corresponding to approximately four d.b.h. (stem diameter at breast height).

During the present study, we first characterized the coarse root architecture of both damaged and undamaged trees and then tested the following hypothesis using a type (3) analysis (see earlier): undamaged trees resisted uprooting both because of preferential root volume allocation to key compartments for stability and because of prevailing wind-oriented root volume reinforcement in these compartments.

Materials and Methods

The stand

The study site was located in the Landes de Gascogne Forest, 60 km south of Bordeaux, France (44°29′43″ N, 0°57′09″ W; 38 m above sea level). The climate is temperate-maritime, with an annual mean temperature of 12.7°C and *c.* 900 mm of annual precipitation. The stand was surrounded by a large area of ploughed land on the north side and by mature *P. pinaster* (Ait.) stands on the other sides. The area was previously a moor on a hydromorphic sandy spodosol, which was drained and afforested towards the end of the nineteenth century. It has a shallow winter water table and experiences water shortage during late summer (Jolivet *et al.*, 2003). Vegetation, soil profile and organic matter storage are markedly affected by seasonal variations in the water table level and by the microrelief. The latter consists schematically in a succession of low ridges and shallow troughs ranging from *c.* 0.3–1.5 m high and 10–50 m wide (Righi & Wilbert, 1984; Jolivet *et al.*, 2003; see Fig. 1). On the better drained, higher parts of the ridges, rooting is halted at a depth of *c.* 0.9 m by an iron pan or a relatively cemented spodic horizon (densic podzol). In the poorly drained troughs, soil profiles have developed in a more humus-rich spodosol, with a friable spodic horizon, locally overlying a hydromorphic Cg horizon (entic podzol). The sides of the ridges exhibit intermediate profiles. The microtopography has not been mapped. For this study, the soil profile and humus content were characterized at 12 random locations in the plot, but individual tree soil profiles were not determined. A 30-m wide track with bilateral 0.9 m deep ditches borders the stand on all sides.

The *P. pinaster* stand covers 62 ha and may have been established in 1950 by broadcast sowing after a forest fire. Since then, systematic thinning has left *c.* 2.5 m wide strips of trees separated by 3.5 m wide strips mechanically weeded before each thinning, which is usually performed every 7 yr. Before the storm, the 50-yr-old single-species stand had reached a mean height of 20.7 m, a 0.38 m mean d.b.h. and a density of 223 trees per hectare. The well-developed undergrowth was cut back between tree strips during the summer of 1999.

Wind direction was monitored on a site 40 km north-east. The prevailing wind came from the west and north-west, and during the storm, the strongest winds came from 235–305°
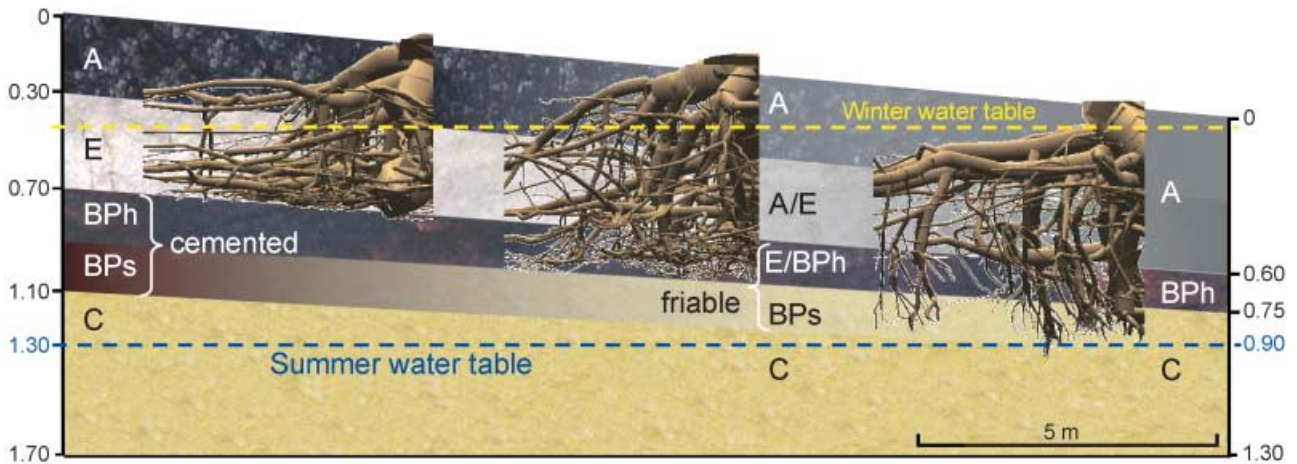
Fig. 1 Diagram of a typical hydromorphic sandy spodosol toposequence with the corresponding rooting patterns. Reconstruction of half the root systems of trees 593, 829 and 363. Toposequence according to Righi & Wilbert (1984) and Jolivet *et al.* (2003). The organic horizon is not represented. The horizontal scale is only for the toposequence. Same horizontal and vertical scale for root systems and the soil depth (m). Horizon names according to the World Reference Base for Soil Resources (WRB, Food and Agriculture Organization of the United Nations, Rome, 1998).

(Cucchi & Bert, 2003). After the storm, a moderately damaged 2.25-ha square plot was selected at 300 m from a clear-cut edge and an inventory of damage was made according to the method described by Cucchi and Bert (2003). On this plot, 10% of the trees were uprooted, levering a root-soil plate from the ground, and 3.6% were inclined. The d.b.h. values of uprooted and undamaged trees did not differ significantly ($P_{Wilcoxon}$ = 0.4). The median directions of uprooting and leaning were 99° and 96.4°, respectively. Aerial photographs showed that a large triangular area starting from the clear-cut edge and oriented NWW suffered 100% windthrow. Thus, the main direction of the wind during the storm was considered to be 276°. The 276 ± 45° quarter will be referred to as the 'windward' quarter. The 'leeward' quarter is its symmetric and the last two quarters were grouped in a discontinuous 'perpendicular to wind' half.

Excavation and 3-D architecture measurement

One undamaged and one uprooted tree per diameter class were sampled in 12 classes in the plot. The north, west and south directions at soil level were tagged by screws driven into the bark and wood. Stem volume was computed from measurements of the height and diameter of all annual growth units (Danjon, 1994). Butt lean value and direction were recorded on undamaged trees, but could not be recorded on uprooted trees. Therefore, the direction of eccentricity and the percentage by which the largest radius exceeded the smallest radius were recorded on stem cross sections sampled at a height of 2.16 m (Stokes & Berthier, 2000). The correlation between eccentricity and the butt angle of lean measured on undamaged trees was 0.8.

The 24 root systems were excavated in May 2000 with a large mechanical shovel, cleaned with a high-pressure air lance

and hand tools and carried to the laboratory. Some broken roots were collected with the mechanical shovel after uprooting, and pasted onto the appropriate areas for measuring, but long shallow roots were not manually excavated, as described in Danjon *et al.* (1999b).

Roots with a base diameter of < 1 cm were removed before measurement. The root systems were positioned outdoors, upside-down, and digitized using a Polhemus Fastrak low magnetic field digitizer (Polhemus, Colchester, VT, USA; http://www.polhemus.com) and DIPLAMI software (Sinoquet & Rivet, 1997). Digitizing consisted of simultaneously recording the topology and XYZ position of measurement points. To gain access to the roots in the middle of root systems, large arborescences were generally cut off when measured.

The root system architecture was measured by starting from the top of the stump and following a recursive path along the branching network. All branching points were thus measured along the root axes. Between branching points, intermediate measurements were performed in order to record changes in both root direction and taper. A segment was defined as the root subdivision between two measured points. The average segment length was 15 cm. When a root cross-section was not circular, the largest diameter and its orientation, as well as the diameter perpendicular to the largest diameter, were recorded. The stump was determined subjectively as the portion of taproot with a large diameter from where most of the large horizontal surface roots originated. The tap root was the largest vertical root originating directly from the stump.

When the sinkers reached the hard pan, they produced several dozen roots running just above it, which were often fused together for their first 0.1–0.5 m in what we called a 'hard pan shield' measuring horizontally up to 0.5 m² (Fig. 2). It was difficult to determine the topology of these structures, so they were considered as a large flat root with branches. Schematically,
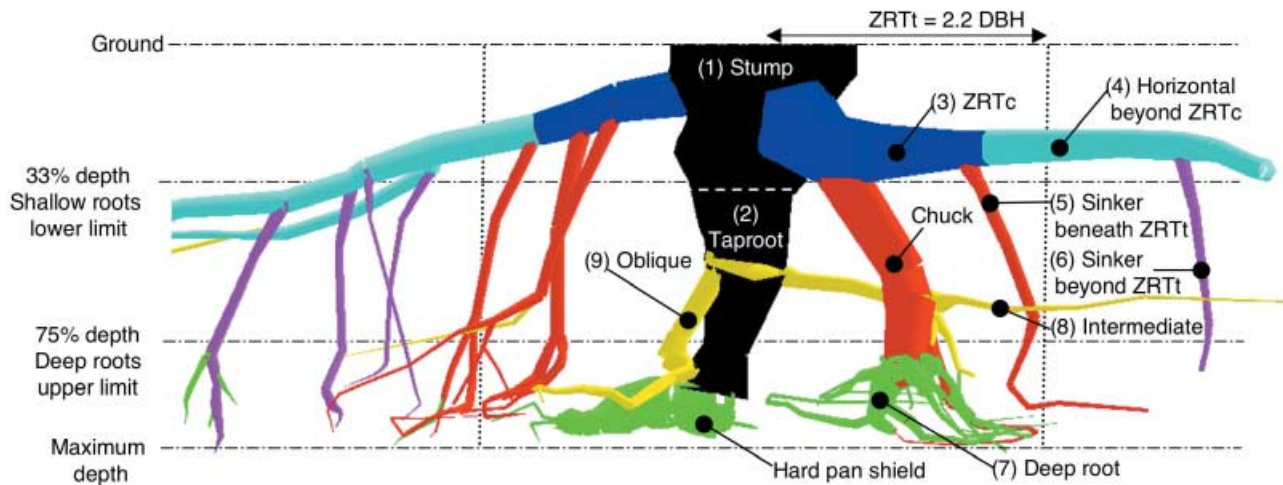
Fig. 2 Schematic representation of the nine compartments and the spatial limits used to determine these compartments. The initial branching point is used to classify the roots as a function of their depth or radial distance, for example, vertical roots (compartments 5 and 6) originate above the deep roots upper limit. All hard pan shield segments are classified in the deep root compartment. Selection of segments in tree 345.

tap roots and sinkers ended in three patterns of deep rooting: (1) abrupt stop with hard pan shield, (2) abrupt stop or (3) brushes (Fig. 3). Using the information provided by the 12 soil profiles available, we hypothesized that these patterns corresponded to the three soil profile classes: ridges with iron pan (four uprooted, seven undamaged trees), sides of ridges (five uprooted, three undamaged trees) and troughs where rooting was stopped by the water table (three uprooted, one leaning, one undamaged tree). Root systems from class (1) were grouped in three ridges, and root systems from class (3) were grouped in two troughs in the stand map. Brushes resulted from the periodical dieback of root tips, with regeneration from existing or new lateral roots (Nicoll & Coutts, 1998). The percentage surface of hard pan beneath the root system was subjectively appraised from examination of the soil on uprooted trees and from the root architecture on undamaged trees.

The 24 trees were ranked according to the influence of a hard pan on their root architecture, defining a 'hard pan score' in the following way: trees exhibiting the deep rooting pattern (3) scored 0. A score of between 5 and 9 was attributed subjectively to the eight trees with deep rooting pattern (2), by examining the way the deep roots stopped their growth. A score of between 14 and 24 was given to the 11 trees with deep rooting pattern (1), as a function of the relative hard pan shield plus deep root graft volume.

Several additional segment features were determined during measurement, including root grafts, lower stump limit, 'hard pan shield' identification and roots ending as a graft in a hard pan shield or in another root.

Characterization of architecture

The characteristics of trees, axes and root segments were computed in the same way as that described in Danjon

et al. (1999a,b), using the AMAPmod software (Godin & Guédon, 1999; Godin *et al.*, 1999; freely available for Linux and Windows platforms: http://www.cirad.fr and ftp://ftp.cirad.fr/pub/amap/AMAPmod; AMAPmod functions for computation of the root characteristics described here are available from the first author) under the Linux Mandrake system. By convention, the tap root was the first order root, roots originating on the taproot were second-order roots, and so on.

Danjon *et al.* (1999a,b) set two fixed spatial limits for shallow and deep roots when studying the vertical distribution of rooting. In the present study, the maximum tree rooting depth ranged from 0.74 to 1.28 m and most vertical roots reached the same depth within a root system. As a consequence, the lower limits for the shallow and upper limits of deep roots were scaled to 33% and 75%, respectively, of the maximum rooting depth beneath the zone of rapid taper (ZRT) for each tree (using ZRTt, see section Root distribution by compartments and Fig. 2).

Only self grafts were observed. Above the deep root limit, the quantity of root grafts was taken into account by the relative sum of half of the bark surface (PsGraft in PCA, see below) of all grafted segments. Below the deep root limit, the percentage of root volume of the hard pan shield and grafted root segments was used.

Root distribution by compartments

Danjon *et al.* (1999a,b) considered that the ZRT included all root segments located within a fixed depth and radial distance of the main tree axis. During the present study, the ZRT compartment (ZRTc) was directly defined from the depth of the axis origin and the taper of the root. The taper of the root cross-sectional area from the axis origin of a segment S included in an axis A was computed as:
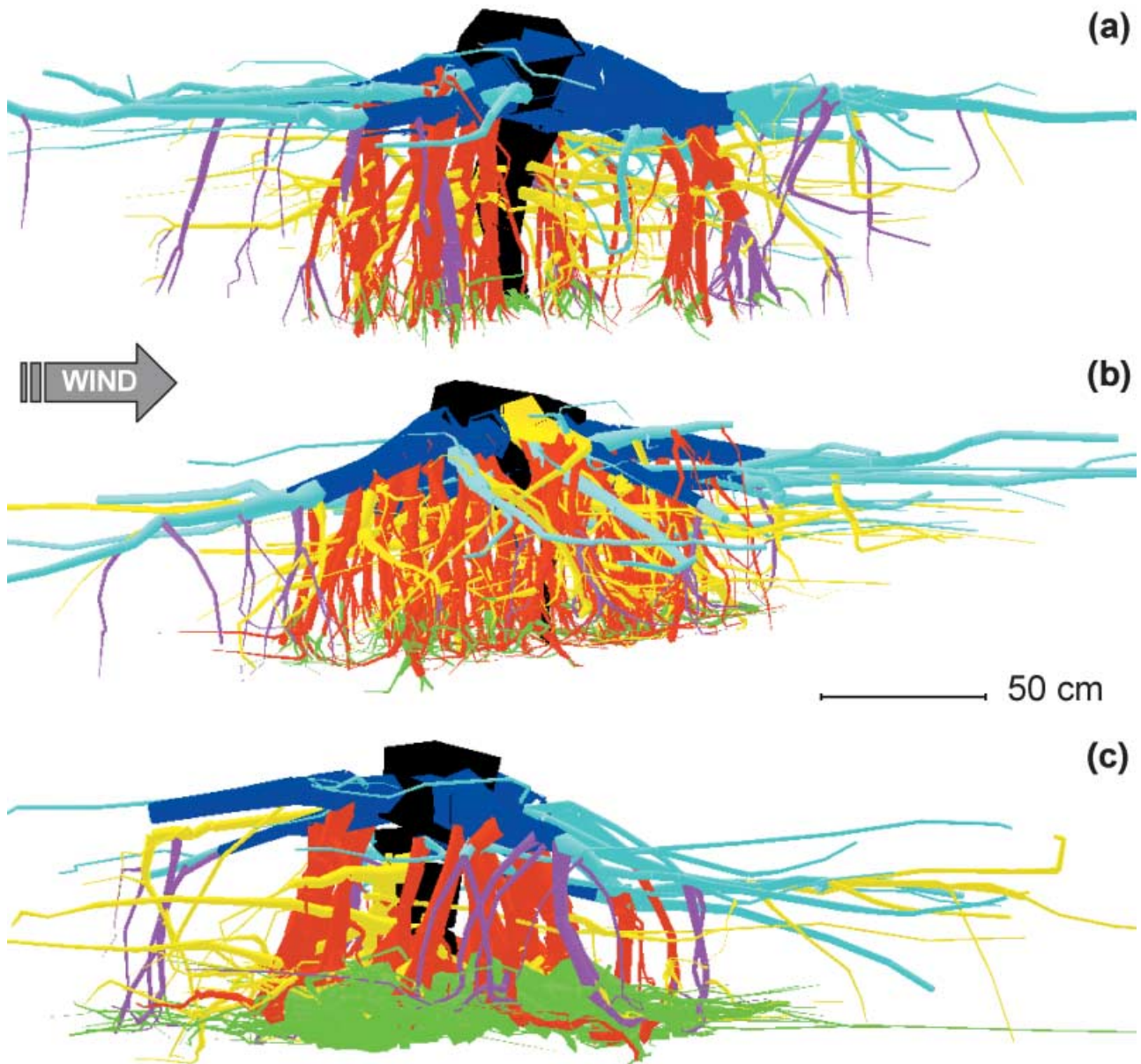
Fig. 3 Vertical reconstruction of three root systems with contrasted deep rooting patterns, with the wind coming from the left. (a) Tree 363 with brushes; (b) tree 30 with abrupt stop; (c) tree 370 with large hard pan shields. Segments were coloured as a function of their compartment (see Fig. 1).

$$CSAtaper_S = ((CSAp_A - CSAd_S)/CSAp_A)/l_{AS}$$

($CSAp_A$ = proximal CSA of axis A; $CSAd_S$ = distal CSA of segment S; l_{AS} = length between the origin of axis A and the end of segment S).

In the context of compartment computations, the ZRTc included the last segment of each axis for which the taper from axis origin was larger than 1.25% per cm and all segments located between the axis origin and this last segment. Root segments were coloured according to their compartment before reconstructing the entire root system as a 3-D image. The taper limit value was then chosen visually depending on the colour of these segments.

Several very large leeward roots tapered very gradually, even when they bore a large number of sinkers. All root segments with a mean diameter larger than d.b.h./5 were therefore included in the ZRTc. An alternative definition of the ZRT was also applied in order to relate it to tree size. Therefore 'ZRTt' was defined as roots originating within a radial distance of 2.2 × d.b.h.

Nine root compartments (Fig. 2) were defined in terms of their location and potential contribution to mechanical resistance. The vertical angle of an axis was generally computed as in Danjon *et al.* (1999a,b) taking −30° and −50° towards the soil surface as the limits between horizontal, oblique and

Table 1 Summary characteristics of the stem and root system of *Pinus pinaster* trees

Variable	Unit	Undamaged mean	SD	Uprooted mean	SD	Difference %	P	r With stemvol	N
Stem eccentricity	%	48.4	25.1	81	38.9	+67%	0.0081	−0.32	
Relative lean direction	degree	19.6	14.2	44.3	30.9	+130%	0.0061	0.1	
Relative CSA of broken ends	%	26	13.5	14.9	16.1	−43%	0.055	0.23	
Crown ratio	%	33.9	5.67	32.3	5.98	−4.7%	0.16	0.62*	n
Stem height	m	20.7	1.32	20.6	0.872	−0.23%	0.45	0.61*	n
Diameter at breast height	cm	37.6	5.04	38.1	5.44	+1.4%	0.25	0.94****	n
Stem volume	m^3	1.01	0.278	1.02	0.292	+1.3%	0.28	1****	n
Stump volume	m^3	0.041	0.016	0.049	0.012	+19%	0.48	0.78***	
Root volume	m^3	0.19	0.079	0.15	0.069	−20%	0.032	0.88****	
Root partitioning coefficient	%	15.7	2.87	13.8	2.11	−12%	0.045	0.35	n
Root length	m	250	74.7	233	93	−6.7%	0.26	0.89****	n
Root maximal radial distance	cm	306	50.1	297	49	−2.9%	0.30	0.67**	n
Stump depth	cm	−32.1	6.22	−35.2	6.79	+9.6%	0.15	−0.17	n
Root maximal depth	cm	−100	11	−98.4	14.2	−1.8%	0.38	−0.34	n
Hard pan score		13.4	9.12	8.58	6.87	−36%	0.063	0.12	n
Root number		476	107	473	164	−0.53%	0.47	0.94****	n
Number of laterals on stump		15	2.63	15.5	6.33	+3.3%	0.41	0.05	n
Fork number		51	87.3	69	54.8	+35%	0.52	−0.09	
Root grafts relative surface	%	4.13	1.6	3.05	1.85	−26%	0.055	0.53*	

When the distribution of variables in both populations was normal (n in the N column), the table shows the mean and SD in both populations, the percentage difference for the uprooted mean and the probability, *P*, of a one-sided paired Fischer test. Conversely, the median and the *P* of a one-sided paired Wilcoxon test are shown. Levels of significance: *, < 5%; **, < 1%; ***, < 0.1%; ****, < 0.01%. *r* with stemvol, correlation with stem volume. Relative lean direction, absolute value of deviation from the windward direction. CSA, cross sectional area.

vertical roots. However, the growth direction of several horizontal surface roots changed to become oblique or vertical at distance from their origin and some sinkers grew horizontally when they reached the hard pan. For the classification of compartments, the vertical angle for horizontal shallow roots and sinkers was therefore computed from their origin to the point were they reached the ZRTt limit or the deep root limit, respectively. The consistency of this classification was checked with AMAPmod on graphs where segments were coloured according to their compartment. The taproot, ZRT and sinkers could form a sort of cage delimited at the bottom by either the brushy lower ends of the tap root and sinkers or by hard pan root proliferations and shields (Figs 2 and 4a).

In most of the root systems, an unusually large leeward third-order root, inclined at *c*. 70° was observed (Fig. 2), and often ended with a shield resting on the hard pan, as a chuck. In 21 trees, the largest second-order root was oriented leeward. In the three remaining trees, it was only the second largest second-order root that was oriented leeward. The largest vertical or oblique third-order root originating from this second-order root was considered as a 'leeward chuck'.

Statistical analysis

Because the stump makes no active contribution to tree stability (Nicoll *et al.*, 1995), it was not used in total root volume computations. The root : shoot ratio was analysed according to

Danjon *et al.* (1999a,b) as a 'root partitioning coefficient' (RPC; i.e. root volume/(root volume + stump volume + stem volume)).

Additional computations, statistics and graphs were produced using the R open statistical package (http://www.r-project.org, functions for root architecture analysis available from the first author). To test differences between uprooted and undamaged tree populations, a Shapiro–Wilk test of the normality of distributions was performed first (Tables 1 and 2). If both populations exhibited normal distributions at the 5% threshold, the mean of both populations and the percentage difference between uprooted and undamaged means were given. Differences were tested using a Fisher pairwise test with trees grouped in pairs of similar stem volume. Conversely, undamaged medians and differences between medians were tested using a Wilcoxon nonparametric pairwise test. One-sided tests were used to determine whether uprooted trees had a significantly larger (or smaller) mean or median compared with undamaged trees.

The circular distribution of the root volume (Table 3) was studied as a proportion of the three wind-oriented sectors described above, within the entire root system, and within compartments. The tap root and root segments located within half of the d.b.h. radial distance were not used in this analysis because their contribution to each sector could not be determined. Undamaged and uprooted trees were tested separately, using the tree as a block factor. The following hypothesis 'At least one proportion is different from at least one other proportion'
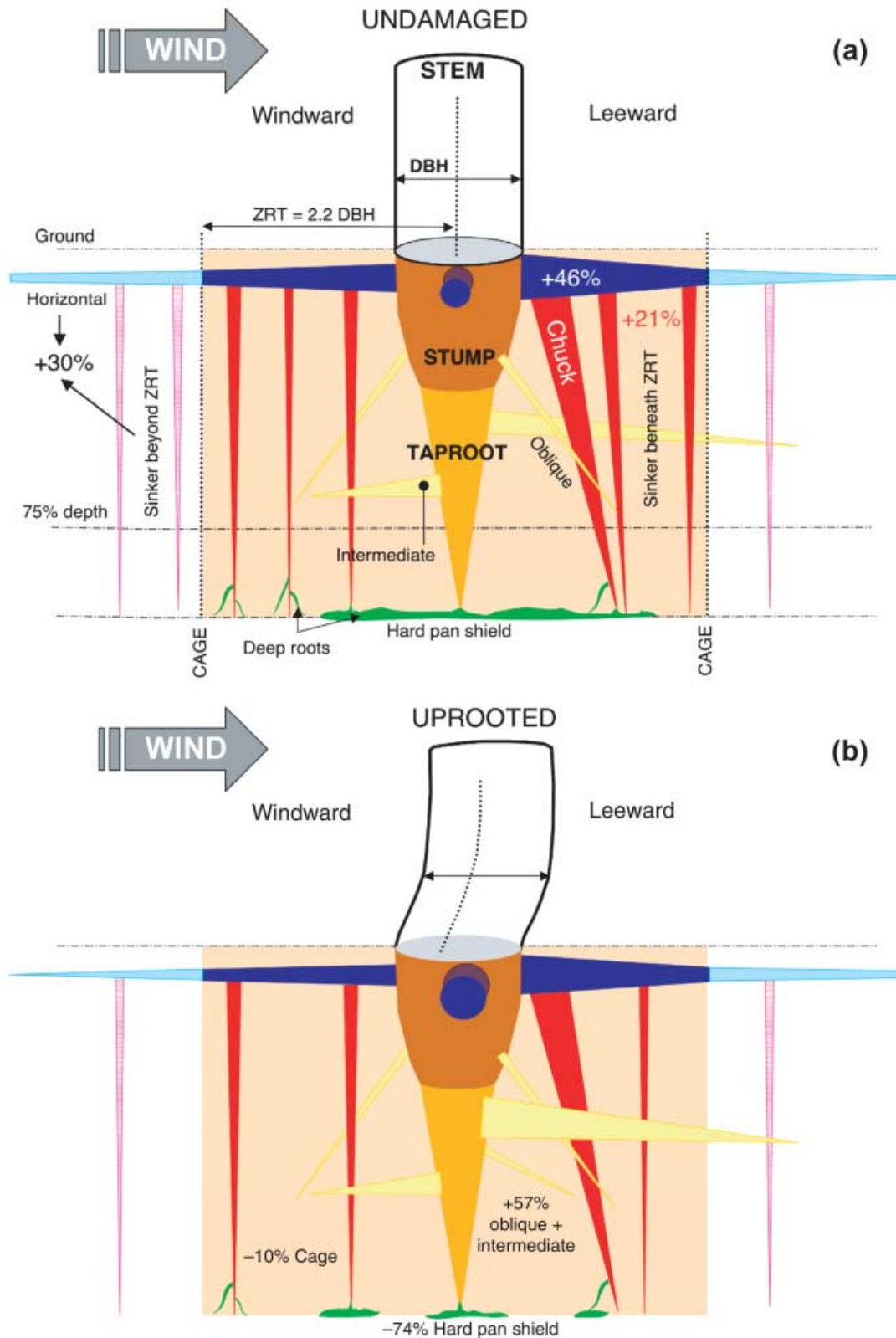
Fig. 4 Schematic representation of mature *Pinus pinaster* root systems grown on sandy spodosol. Root number and size is arbitrary.
(a) Undamaged tree, the percentages refer to the prevailing wind oriented reinforcement in the corresponding compartments. (b) Uprooted tree, the percentages refer to the difference in root volume proportion compared with undamaged trees; uprooted trees exhibited wind-oriented reinforcement only in the intermediate and oblique roots compartment (+50% leeward).

Table 2 Root volume proportion in the nine compartments and for deep grafts and shields, chuck and cage as a percentage of the root system volume, stump excluded, except for the first variable

Variable	Undamaged mean	SD	Uprooted mean	SD	Difference %	P	r With stemvol	N
(1) Stump	19.9	5.75	22.6	6.78	+14%	0.21	−0.38	n
(2) Taproot	7.52	3.8	8.96	6.34	+19%	0.26	−0.42	n
Deep grafts and shield	6.37	11.2	1.63	3.35	−74%	0.046	−0.21	
Chuck	11.8	5.44	10.7	4.63	−9.1%	0.32	−0.61*	n
Chuck weighted by direction	8.27	4.47	7.67	4.81	−7.3%	0.39	−0.5*	n
Vertical component of chuck	2.63	2.22	3.38	2.1	+28%	0.40	−0.34	
(3) ZRTc	27.2	9.15	28.8	6.12	+5.9%	0.32	0.17	n
(4) Horizontal shallow beyond ZRTc	13.2	5.17	12.8	4.37	−3.3%	0.41	0.51*	n
(5) Sinkers beneath ZRTt	21.5	3.79	17.8	6.11	−17%	0.070	−0.2	n
(6) Sinkers beyond ZRTt	2.91	1.8	2.98	1.14	+2.2%	0.46	0.26	n
(7) Deep roots	14.1	13.6	7.57	4.82	−46%	0.072	−0.21	n
(8) Intermediate	10.1	5.24	15.2	6.67	+50%	0.024	0.15	n
(9) Oblique	2.96	2.38	6.4	4.32	+120%	0.055	−0.14	
Cage = (2) + (3) + (5) + (7)	69.7	7.82	62.4	6.95	−10%	0.0023	−0.48	n

When the distribution of variables in both populations was normal (n in the N column), the table shows the mean and SD in both populations, the percentage difference for the uprooted mean and the probability, P, of a one-sided paired Fischer test. Conversely, the median and the P of a one-sided paired Wilcoxon test are also shown. ZRTc, zone of rapid taper of horizontal shallow roots defined from the taper; ZRTt, $2.2 \times$ d.b.h. radial distance.

Table 3 Undamaged and uprooted *Pinus pinaster* trees: (1) circular distribution of root volume in several compartments and (2) circular distribution of root length and root number, deep roots being excluded

Compartments	Undamaged					Uprooted				
	P	ww	pp/2	lw	N	P	ww	pp/2	lw	N
(1) Per cent volume in the corresponding compartments										
Total	0.017	26ab	21b	31a		0.034	24b	23b	31a	n
ZRTc	0.028	22b	21b	37a		0.054	20	23	35	n
Intermediate and oblique	0.47	27	24	25		0.0018	28b	17c	38a	
Sinkers beneath ZRT	0.040	26ab	22b	30a	n	0.87	27	24	26	n
Deep roots	0.34	22	23	33		0.93	25	24	27	n
Beyond ZRT	0.049	32a	20b	27ab	n	0.64	23	22	28	n
(2) Per cent root length and number excluding deep roots										
Root number	1.10^{-6}	33a	23b	20b	n	0.083	32	22	23	n
Root length	3.10^{-6}	32a	23b	21b	n	0.34	30	23	23	

P is the probability associated with either a two-way ANOVA for normally distributed variables (n in the N column) or with a Friedman test. Different letters indicate significant differences using multiple comparison procedures. ww, windward quarter; pp/2, half the discontinuous 'perpendicular to wind' half; lw, leeward quarter. ZRT, zone of rapid taper.

was tested. For normally distributed variables, a two way analysis of variance and a Tukey multiple comparison procedure was used ('simtest' in R). Alternatively, a Friedman nonparametric test and its associated multiple comparisons procedure was used (Sprent, 1989). The volume reinforcement of a sector was computed using the following formula: (%volume − 25%)/25%.

A principal component analysis (PCA) of the 24 trees was made using 21 variables. Overturning is mainly due to wind loading on the crown and to the displacement of weight from the stem to the crown (Faure & Pelet, 1984). For this reason, most of the root architecture parameters dependent on tree size were analysed as a percentage of stem volume (variable name starting with the letter S), and are referred to as the 'relative root volume'. Some of them were also studied as a percentage of the total root volume without the stump (variable name starting with the letter P). Compartments 5 and 6 (sinkers) and 8 and 9 (intermediate depth and oblique roots) were, respectively, pooled together. The percentage of very large roots in a root system (Pverylarge) was computed using the cubic root of stem volume divided by 20 as the lower diameter limit, so as to scale this variable to the size of the tree.

Results

General stem and root system characteristics

Undamaged trees showed a 48% average stem section eccentricity compared with 81% of uprooted trees, which certainly results from the stem having been inclined at a greater angle in the past (Table 1). Nine uprooted trees had an eccentricity exceeding 70%, whereas only one undamaged tree (tree 768) exceeded 79% eccentricity and exhibited a 15° angle of inclination after the storm. Moreover, uprooted trees generally did not show any leeward oriented eccentricity (i.e. they did not lean in a leeward direction before storm). From a qualitative examination of growth ring series, it appeared that the stem base eccentricity of uprooted trees had started at approx. 5–10 yr of age.

A potential bias due to root breakage during windthrow was assessed through the CSA of all broken root ends with an end diameter of > 1 cm, divided by the stem cross-sectional area at breast height. Uprooted and undamaged trees did not differ for that variable, so that uprooted and undamaged trees could be analysed on the same basis. Furthermore, the mean maximum radial distance of roots reached 3 m in both cases.

The root partitioning coefficient (RPC) averaged 16%. Uprooted trees exhibited a 20% lower root volume and a 12% lower RPC. The quantity of root grafts above the deep root limit reached 4% of the root external area. Differences in the hard pan score and root grafts were nearly significant ($P = 0.063$ and $P = 0.055$, respectively). Uprooted trees did not differ significantly from undamaged trees in terms of either stem size variables or root spatial extension and root branching variables. Neither RPC nor maximum root depth were related to stem size.

Root volume distribution by compartments

In undamaged trees, the stump comprised 20% of the total excavated coarse root volume (Table 2, Fig. 4a). The tap root proportion was 7.5% of root volume. The relative volume of hard pan shield and deep root grafts reached 6.5%, but among the 20 trees growing over a hard pan, only seven undamaged trees and five uprooted trees exhibited a hard pan shield, the corresponding median proportion for these trees being 10.5%. The leeward chuck was a large structure corresponding to 12% of the root volume, its sinker component averaging 2.6% of the root volume, which was one-third of the tap root. The ZRT and sinkers beneath the ZRT were the most important compartments, averaging 27% and 22% of the root volume, respectively. Horizontal surface roots beyond the ZRT and deep roots scored 13% and intermediate horizontal roots constituted 10% of the root volume. The proportion of sinkers beyond the ZRT and of oblique roots was lower than 3%. The 'cage' formed by the ZRT, taproot, sinkers and deep roots beneath the ZRT comprised 70% of the root volume.

Uprooted trees exhibited a 10% and 74% lower root volume proportion in the cage and in the hard pan shield, respectively (Table 2, Fig. 4b). They showed a 50% larger root volume proportion in the intermediate depth root compartment. Differences regarding sinkers beneath the ZRT (−17%), deep roots (−46%) and oblique roots (+120%) were nearly significant ($P < 0.075$). When the root volume in the compartment was analysed as the relative root volume (per cent of stem volume – not shown), the difference between uprooted and undamaged trees reached −29% ($P = 0.057$), −56% ($P = 0.052$) and +64% ($P = 0.059$) for sinkers beneath the ZRT, deep roots and oblique roots, respectively. Only undamaged trees (eight trees) had a relative cage volume above 13.5%, while only uprooted trees (4 trees) had a relative cage volume below 10%.

Root volume distribution by circular sector

In undamaged trees, the differences in root volume within the three wind-oriented sectors defined above were significant in the whole root system, in the ZRTc as well as in sinkers beneath the ZRT and in roots beyond the ZRT (Table 3, Fig. 4a). The deep, intermediate and oblique root compartments did not demonstrate any circular heterogeneity. When the whole root system was considered, only the leeward quarter showed a 26% volume reinforcement at the expense of perpendicular to wind quarters. As expected, the ZRT was only and strongly (46%) reinforced in the leeward quarter, being associated with a 21% leeward volume reinforcement in sinkers beneath the ZRT. Conversely, the roots beyond the ZRT (which mainly consisted of horizontal shallow roots) showed a 30% windward reinforcement. The distribution between (leeward + windward) vs perpendicular to wind root volume was generally close to a ratio of 60/40. In all undamaged trees, the root volume of each wind oriented circular quarter was between 12.5% and 40%, and was always larger than 25% in the leeward quarter.

Root length and root number circular distribution were highly reinforced in the windward quarter (+28% and +32%, respectively).

Uprooted trees showed a lower heterogeneity in the circular distribution of the ZRTc and total root volume, and no circular heterogeneity in deep roots, sinkers and roots beyond the ZRT. However, they exhibited a high level of heterogeneity in terms of intermediate depth and oblique root compartment circular distribution, with a 52% leeward and 12% windward reinforcement but a weak windward reinforcement of root length and number (Table 3, Fig. 4b).

Multivariable comparisons of trees

The first two components of the PCA on individual tree characteristics explained 39% of variance (Fig. 5). High positive loadings for the first component (PC1) corresponded to trees having a large size and windward reinforcement, a high proportion of root grafts and shallow root volume beyond the
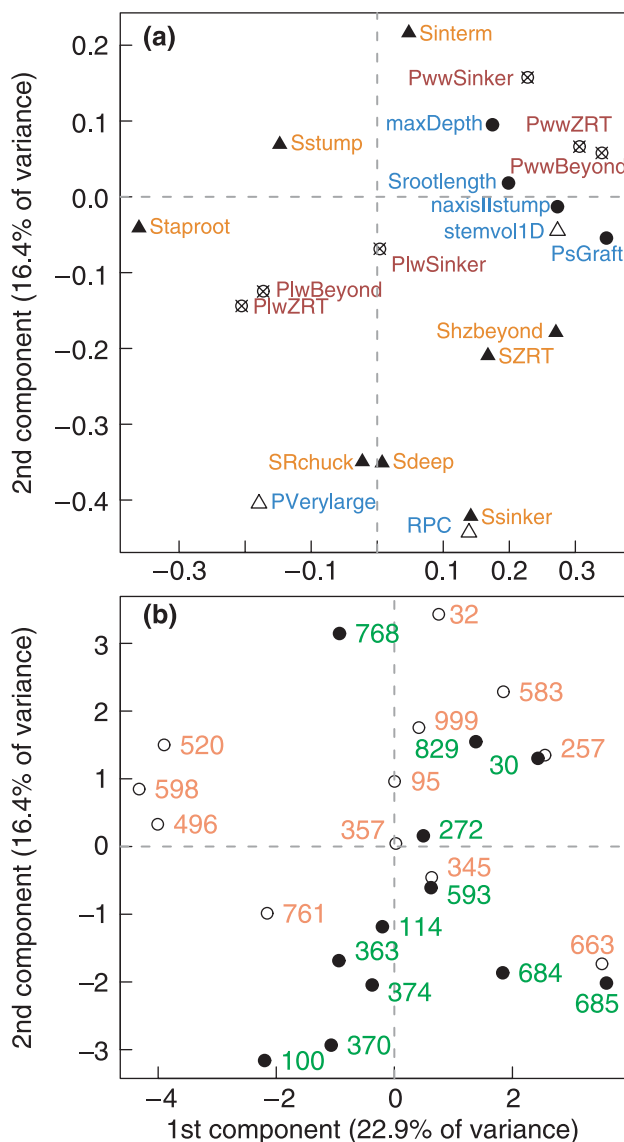
Fig. 5 Principal component analysis (PCA) of tree characteristics. Scores for PC1 and PC2. (a) Loadings for the 21 original variables: open triangles, volume variables (stemvol1D = cubic root of stem volume); closed triangles, compartment volume as a percentage of stem volume (Sstump, stump; Staproot, taproot; Sinterm, oblique and intermediate depth; SZRT, ZRTc; Shzbeyond, horizontal shallow roots beyond ZRTc; Ssinker, sinkers; Sdeep, deep roots; Srchuck, vertical component of the leeward chuck weighted by direction); crossed circles within squares, percentage of root volume in the windward (ww) and leeward (lw) quarter in ZRTc, sinkers beneath ZRTt and roots beyond ZRTt; closed circles, other variables (maxDepth, maximum rooting depth; naxisIIstump, number of second order root branching from the stump; Srootlength, root length divided by stem volume). (b) Loadings for the 24 trees of the sample. Closed circles, undamaged; open circles, uprooted.

None of the undamaged trees was located above the bisecting line, and none of them exhibited high negative loadings for PC1 or high positive loadings for PC2, except for leaning tree 768. Most of the undamaged trees showed a high RPC and a high relative cage volume, but not trees 768, 829, 30 and 272.

Uprooted trees 496, 520 and 598 with large negative loadings on PC1 and small positive loadings on PC2 had a marked rooting depth, a low relative deep root volume and no hard pan shield, but a very large relative tap root volume. This indicates that they were located in shallow troughs. They had all < 11% of their root volume beyond the ZRT located windward. These trees also exhibited to varying degrees a deficit in the ZRT, sinkers, horizontal roots beyond the ZRT, the windward ZRT and leeward or windward sinkers, resulting in a very low RPC, stump and taproot excluded. They also showed a low root length, root graft surface and number of second-order roots on the stump. It is hypothesized that waterlogging in the troughs resulted in the poor development or dieback of second order roots on the stump (especially windwards), involving a weak circular distribution and resource reallocation from most compartments to the stump and taproot.

Uprooted tree 32 and leaning tree 768, and to a lesser extent uprooted tree 999 with small loading on PC1 and high positive loading on PC2, showed a low RPC even when stump was included, and a generally weak development of different elements of the 'cage', but a medium relative volume in intermediate depth roots. On one hand they had all a large number of second-order roots on the stump, but on the other hand, they had a moderately inappropriate root circular distribution with a weak leeward horizontal relative root volume.

Eight trees (undamaged trees 829, 30 and 272 and uprooted trees 257, 345, 357, 583 and 95) had small positive loadings on both PC1 and PC2 and therefore median characteristics for most of the variables used in the PCA, but they had all a low deep root relative volume, growing over 70–100% of hard pan. Their relative cage volume was between 10% and 12%.

Uprooted tree 663 and undamaged tree 685 exhibited fairly similar loadings in the first four PCAs and therefore displayed a similar size and architecture. They were very large trees with large RPCs growing in relatively shallow soil (95 cm). However, tree 663 scored 13.3% for its relative cage volume vs 16% for tree 1685, and had an exceptionally small proportion of leeward root beyond the ZRT (2.4%).

In the PCA, trees with deep roots ending in brushes are mostly located towards negative loadings for PC1 and positive loadings for PC2, whereas trees showing an abrupt stop with a hard pan shield were mostly located towards positive loadings for PC1 and negative loadings for PC2. Trees with an abrupt stop without a shield were in between. Thus, trees on ridges had a higher RPC, and more roots in all compartments, except for intermediate depth and stump, and had small taproots.

PC3 (13.3% of variability – not shown) mainly highlighted the exceptional root length and relative volume of intermediate depth roots in uprooted trees 583 and 761 and undamaged

ZRT and a small taproot. Large negative loadings for PC2 corresponded mainly to trees with a large RPC due to large sinkers, leeward chuck and deep root volume, and a high proportion of thick roots.

tree 593, with the lowest rooting depth (0.74, 0.80 and 0.80 m maximum rooting depth, respectively). Undamaged tree 593 had a 16% relative cage volume vs 10.3% and 12.7% for uprooted trees 583 and 761, respectively.

Discussion

The typical *P. pinaster* root system is highly structured and efficient for anchorage

Mature *P. pinaster* trees growing on sandy spodosol exhibited a strong organization of root system architecture (Fig. 4a) and high variability for several of their features, which partly originates from their adaptation to a broad range of soil profiles. Their root systems differ radically from a heart root system (Köstler *et al.*, 1968; Stokes, 2002) because of the very small proportion of oblique roots at shallow or intermediate depth and a large volume of sinkers. The taproot thus averaged 7.5% of root volume in 5-yr-old planted *P. pinaster* growing in a similar soil (Danjon *et al.*, 1999a,b). It ranged broadly from 1.5% to 14% in these mature trees. The taproot plays an important role in seedling and sapling stability, where it acts as a pole in the soil (Danjon *et al.*, 1999b). It is gradually relayed in older trees, vertical anchorage being reinforced by secondary sinkers whose mean volume averages three times the tap root volume in mature trees. The taproot then contributes with ZRT and sinkers to the rigidity of the entire root soil plate. When the taproot has reached soil layers impervious to roots, there is a threshold where an additional biomass allocation to the taproot will not provide an additional contribution to anchorage. The development of other compartments of the cage may compensate for poor taproot development: undamaged tree 685 had a taproot proportion of < 2.5%, but a large RPC and cage. In any case, the taproot is a minor component in mature root systems. In the same way, the proportion of stump was not related to wind-firmness despite broad variability, but it was related to maximum rooting depth.

The ZRT is an important below-ground carbon sink corresponding to more than one-quarter of the root volume, and nearly four times the tap root volume. The sinker volume was mainly located within twice the d.b.h. radial distance, forming a solid cage with the ZRT, which rarely broke during uprooting, firmly holding the corresponding soil mass in place. It corresponded approximately to the root soil plate radius, which averaged 2.2 × d.b.h. in uprooted trees. The lateral movement of shallow horizontal roots is hampered by the large number of sinkers branching from the ZRT. In half the trees, the bottom of the cage was locked by a large quantity of deep roots, mainly below the ZRT. It could even be locked by a set of hard pan shields which attained one third of the root volume in one tree. It is not known whether the proportion of hard pan shield results from soil conditions or the genetic characteristics of trees. Half of the uprooted trees may have failed principally because of weakness of the cage, either because it had large openings,

or because it was weak, with a small volume of sinkers and deep roots. The enclosed soil volume adhering to inner roots in the cage may contribute to root anchorage, increasing the root-soil plate weight. Trees that develop rigid root-soil plates through adaptive growth of their structural roots increase the contribution of soil resistance to overturning (Ray & Nicoll, 1998). Greater stiffness of a larger root-soil plate ensures smaller displacement sooner during uprooting and may prevent initial failure in the soil (Coutts, 1986). In was found that during prevailing wind-oriented winching tests on *P. pinaster* the critical loading point was reached at the beginning of the test, when stem inclination was small, especially in older trees (Cucchi *et al.*, 2004). This suggests that soil resistance, and therefore root-plate rigidity, plays a key role during this early stage. According to Ennos (1993), plate root systems become more efficient than taproot root systems at large plant sizes because the anchorage provided by the weight of the root soil plate rises with the fourth power of linear dimensions. Dupuy *et al.* (2005b) showed that deep vertical roots play a major role in sandy soil. Mature trees have a large number of self root grafts providing an additional rigidity to the cage. The low rooting depth and structure of *P. pinaster* root systems result in zones with a high root density, increasing the probability of a root coming into contact with another root to form a graft. Furthermore, a greater development of intermediate roots and tap root cannot compensate for weak cage development. Intermediate roots may not have the same efficiency in holding the tree: since they are not attached to the large stump they generally do not bear sinkers and do not have an even circular distribution. Horizontal roots beyond the ZRT certainly play an important role in the exploration and exploitation of surface water and nutrients, and they act also as guys, under tension, to hold the upper surface of the cage.

Most temperate conifers develop roughly the same type of coarse root architecture as *P. pinaster* (e.g. Coutts *et al.*, 1990; Watson & O'Loughlin, 1990; Drexhage & Gruber, 1998) which is dependent upon the soil depth available, the slope and intertree competition. *Pinus pinaster* in a sandy podzol may stand out because of its exceptionally large volume proportion in sinkers beneath the ZRT, its ability to develop large hard pan shields and the absence of intertree root grafts.

In half of the uprooted trees, damage obviously originated from a weak RPC and root architecture (Fig. 4b). The RPC may partly be under genetic control (Wu & Yeh, 1997). Trees 583 and 761 may have failed because of a shallow hard pan and tree 663 because of a very large stem volume, which were not compensated by an exceptional root architecture. However, five uprooted and three undamaged trees had average root system characteristics: their resistance to uprooting may have been determined by their position in the stand, their aerial architecture or by characteristics not taken into account in the present study. They could also have been struck by a neighbouring tree. An estimation of tree characteristics at the stand level can be made, based on the fact that damaged trees

represented 10% of this tree population and undamaged trees 90%: 4.6% of the trees failed because of defective root systems, 2.3% because of very low rooting depth or size not compensated by root design, 65.5% of the trees had reinforced root systems, 24.5% had medium root characteristics and did not fail and 3.1% had medium rooting characteristics and failed.

Pinus pinaster exhibits a broad structural adaptation to soil conditions

In the *P. pinaster* root systems observed, rooting depth was related to relative stump and tap root size ($r = 0.6**$), but neither to wind-firmness, stem volume nor another compartment volume. Nevertheless, trees with greater rooting depth are expected to be larger, because of better access to water and nutrients (Bréda *et al.*, 1993). Several trees exhibited a very high number of entangled fine roots growing directly over the hardpan in a kind of 2–4 cm thick 'hard pan root mat', which was also located mostly beyond the ZRT. This mat certainly plays a major role in the water and nutrient acquisition of trees growing over a hard pan. When taproot penetration is abruptly stopped by the hardpan, trees reallocate resources from the taproot and stump to alternative compartments, as observed by McMinn (1963) in *Pseudotsuga menziesii*. Thus, within the 0.85–1.3 m maximum rooting depth range, the tree adapts its root system in different ways using the available soil depth. However, there may be a threshold above a depth of 0.85 m where trees develop longer roots and a larger number of intermediate depth roots. In our study, the five trees with a typical brushy deep root pattern had a mean rooting depth of 1.11 m, while trees stopped by the hard pan averaged a 0.96 m rooting depth ($P_{wilcoxon} = 0.015$). It is assumed that the fairly deep hard pan (0.75–1.1 m) had a positive effect on wind-firmness, providing a highly stable support to vertical roots. Stability was then further reinforced by the development of a leeward chuck, ending in a hard pan shield. By contrast, root systems whose vertical growth was only halted by the water table benefited from weaker support that was not compensated by the 15% larger mean rooting depth or by increased branching of the deepest roots. In addition, their location in poorly drained shallow troughs was generally associated with waterlogging and root decay. In a previous tree winching study, Cucchi *et al.* (2004) found no effect of the presence of a hard pan on the critical overturning moment of *P. pinaster* trees growing in the Landes de Gascogne forest.

Wind-firmness is improved by a selective reinforcement in the prevailing wind direction

Globally, undamaged trees exhibited an even circular distribution of roots associated with a selective volume reinforcement in sectors parallel to the wind. Tree root systems often display a remarkably uneven development (Nicoll *et al.*, 1995). However, high circular distribution asymmetry has mainly been found in stand with asymmetric intertree competition (i.e. mixed species, uneven-aged, extensively managed stands) (Eis, 1974; Watson & O'Loughlin, 1990). Leeward reinforcement of the ZRT and sinkers corresponds partly to the horizontal and vertical component of the above-mentioned 'leeward chuck' providing a direct counterbalance to wind effect, whereas the tap-root resists by acting as a lever arm. Nicoll & Dunn (1999) reported that in shallow-rooted 46-yr-old *P. sitchensis*, the amount of secondary thickening in any part of the root system in any one year was proportional to the amount of stress experienced at that point. Therefore, our result concerning selective circular reinforcement suggests that two areas of the root system experienced the greatest stress:

1 the leeward ZRT and sinkers beneath the ZRT,
2 the windward shallow and sinker roots beyond the ZRT.

The number of roots was higher and root length was longer on the windward side, where the roots were under tension during wind loading. Tension is transferred to the soil via friction, so that a large root surface area on the windward side, over which the load can be distributed, is beneficial to tree anchorage (Stokes *et al.*, 1996). Furthermore, roots with a smaller diameter are more resistant to tension than bigger roots (Genet *et al.*, 2005). Conversely, on the leeward side, despite a large volume reinforcement, root numbers were no higher and roots were no longer. Under wind loading, leeward roots are mainly placed under compression or bending. The stiffness of a root with a circular section is proportional to the fourth power of the diameter, and resistance to breakage is proportional to the third power of the diameter (Coutts, 1987). Thus, in order to obtain effective support, trees develop one or two very large second order horizontal leeward roots which taper very gradually. This is a structural adaptation which enlarges the turning moment for uprooting and root-soil plate rigidity by increasing the radial distance of the root-soil plate hinge (Coutts, 1987). Roots perpendicular to the direction of displacement are held in torsion and offer little resistance to uprooting (Stokes, 2002).

Using winching tests, Coutts (1986) showed that in 35-yr-old *P. sitchensis* planted on turfs alongside a plough furrow, soil resistance contribute considerably to anchorage, but only at the very beginning of uprooting. At the critical loading point, counter-winchward roots represented 55% of the turning moment while values reached 30% for the root-soil plate mass and only 8% for the winchward hinge and soil resistance. Crook & Ennos (1996) found a 25% contribution of winchward roots to anchorage in 15 cm d.b.h. deep rooted *Larix* trees. In addition, only the area of counter-winchward laterals and winchward sinkers 10 cm along their length was correlated to anchorage strength. However, in Coutts' (1986) study, plough furrows restricted root growth, and in the Crook & Ennos (1996) study, the trees uprooted without root-soil plates. Moreover, in both publications, as in almost all of the papers on winching experiments published to date, the trees were not pulled in the direction corresponding

to the prevailing wind. Under Atlantic wind regimes, the possibility of wind-blow occasioned by storms from an unusual direction is low (O'Cinnéide, 1975). Thus the contribution of the leeward ZRT and sinkers to wind-firmness in *P. pinaster* is likely to be substantially greater than the contributions determined in both of the aforementioned publications. More generally, trees along the Atlantic seaboard of western Europe are likely to improve their survival and therefore the number of their offspring through a prevailing wind-oriented selective reinforcement of key compartments for stability. In this context, random oriented winching tests probably underestimated the measurements of critical turning moments.

Pinus pinaster cannot develop strong anchorage from a defective juvenile root system

Heart root systems may be able to compensate for a weak circular distribution in surface roots because of the spatial distribution of second-order roots. In addition, some species such as *Platanus hybrida* constantly form new roots on the stump and show very frequent forking (Atger & Edelin, 1994). By contrast, *P. pinaster* has a sinker root system, a low forking rate and apparently cannot easily regenerate new roots in the vicinity of the stump. Therefore, when a *P. pinaster* tree has not developed an evenly distributed array of shallow roots at the seedling stage, it cannot regenerate an appropriate shallow root array bearing an evenly distributed set of sinkers and deep roots at the sapling stage; it has also been shown that compensatory development of the tap root and intermediate depth roots cannot provide efficient anchorage. If a root forks into two branches of even size with a total CSA equal to that proximal to the fork, then the total stiffness of the roots will be halved (Coutts, 1983a). In *P. pinaster*, a low forking rate is therefore associated with the good mechanical resistance of roots. On the other hand, the numerical calculations carried out by Dupuy *et al.* (2005a) showed that forking, or to a lesser extent branching, can significantly increase the pull-out resistance of roots by increasing root–soil interactions.

Conclusion

Our results as a whole confirm previous observations concerning a possible biomechanical adaptation of the root system to the prevailing wind in trees resistant to wind. In *P. pinaster*, the most resistant root architecture design appears to be the undisturbed development described above (Fig. 4a), adapted to the soil conditions available. Mature trees have a taproot/ sinkers root system. The stem is mainly anchored on the ground by a large, leeward, reinforced root cage forming a broad and rigid soil plate which is firmly anchored by windward reinforced shallow roots. This pattern may be altered (Fig. 4b) by waterlogging, competition or establishment techniques (Danjon *et al.*, 1999b). The straightforward relationships usually observed between stability and both the soil depth

available and the occurrence of a hard pan were not found during the present study. The hard pan certainly provides a firm support for the root system and microtopographic sequences associate greater soil depth and an absence of hard pan to waterlogging. Finally, in climates where the direction of catastrophic wind-blows is close to the prevailing wind direction, trees can improve their stability through prevailing wind-oriented selective reinforcement.

References

Atger C, Edelin C. 1994. Premières données sur l'architecture comparée des systèmes racinaires et caulinaires. *Canadian Journal of Botany* **72**: 963–975.

Blackwell PG, Renolls K, Coutts MP. 1990. A root anchorage model for shallowly rooted Sitka spruce. *Forestry* **63**: 73–91.

Bréda N, Cochard H, Dreyer E, Granier A. 1993. Water transfer in a mature oak stand (*Quercus petraea*): seasonal evolution and effects of a severe drought. *Canadian Journal of Forest Research* **23**: 1136–1143.

Butnor JR, Doolittle JA, Kress L, Cohen S, Johnsen KH. 2001. Use of ground-penetrating radar to study tree roots in the southeastern United States. *Tree Physiology* **21**: 1269–1278.

Coutts MP. 1983a. Development of the structural root system of Sitka spruce. *Forestry* **56**: 1–16.

Coutts MP. 1983b. Root architecture and tree stability. *Plant and Soil* **71**: 171–188.

Coutts MP. 1986. Components of tree stability in Sitka spruce on peaty gley soils. *Forestry* **59**: 173–197.

Coutts MP. 1987. Developmental process in tree root systems. *Canadian Journal of Forest Research* **17**: 761–767.

Coutts MP, Walker C, Burnand AC. 1990. Effect of establishment method on root form of lodgepole pine and Sitka spruce on the production of adventitious roots. *Forestry* **63**: 143–159.

Coutts MP, Nielsen CCN, Nicoll BC. 1999. The development of symmetry, rigidity and anchorage in the structural root system of conifers. *Plant and Soil* **217**: 1–15.

Crook M, Ennos A. 1996. The anchorage mechanics in deep rooted larch, *Larix europea* × *L. japonica*. *Journal of Experimental Botany* **47**: 1509–1517.

Cucchi V, Bert D. 2003. Wind-firmness in *Pinus pinaster* Ait. stands in southwest France: influence of stand density, fertilisation and breeding in two experimental stands damaged during the 1999 storm. *Annals of Forest Science* **60**: 209–226.

Cucchi V, Stokes S, Meredieu C, Berthier S, Najar M, Denis A, Lastennet R. 2004. Root anchorage of inner and edge trees in stands

of Maritime pine (*Pinus pinaster* Ait.) growing in different podzolic soil conditions. *Trees – Structure and Function* **18**: 460–466.

Danjon F. 1994. Heritabilities and genetic correlations for estimated growth curves parameters in maritime pine. *Theoretical and Applied Genetics* **89**: 911–921.

Danjon F, Bert D, Godin C, Trichet P. 1999a. Structural root architecture of 5-year-old *Pinus pinaster* measured by 3D digitising and analysed with AMAPmod. *Plant and Soil* **217**: 49–63.

Danjon F, Sinoquet H, Godin C, Colin F, Drexhage M. 1999b. Characterisation of structural tree root architecture using 3D digitising and AMAPmod software. *Plant and Soil* **211**: 241–258.

Drexhage M, Gruber F. 1998. Architecture of the skeletal root system of 40-year-old *Picea abies* on strongly acidified soils in the Harz Mountains (Germany). *Canadian Journal of Forest Research* **28**: 13–22.

Dupuy L, Fourcaud T, Stokes A. 2005a. A numerical investigation into factors affecting the anchorage of roots in tension. *European Journal of Soil Science* **56**: 319–327.

Dupuy L, Fourcaud T, Stokes A. 2005b. A numerical investigation into the influence of soil type and root architecture on tree anchorage. *Plant and Soil.* (In press.)

Eis S. 1974. Root system morphology of western hemlock, western red cedar, and douglas-fir. *Canadian Journal of Forest Research* **4**: 28–38.

Ennos AR. 1993. The scaling of root anchorage. *Journal of Theoretical Biology* **161**: 61–75.

Faure A, Pelet J. 1984. Détermination des efforts exercés par le vent sur un arbre. *Agronomie* **4**: 83–90.

Fourcaud T, Dupuy L, Sellier D, Ancelin P, Lac P. 2003b. Application of plant architectural models to biomechanics. In: Hu BG, Jaeger M, eds. *Plant Growth Modeling and Applications – Proceedings PMA03.* Beijing, China: Tsinghua University Press and Springer, 462–479.

Genet M, Stokes A, Salin F, Mickovski SB, Fourcaud T, Dumail J, van Beek R. 2005. The influence of cellulose content on tensile strength in tree roots. *Plant and Soil.* (In press.)

Godin C, Guédon Y. 1999. *AMAPmod v1.8. Introduction and reference manual.* Montpellier, France: CIRAD.

Godin C, Guédon Y, Costes E. 1999. Exploration of plant architecture databases with the AMAPmod software illustrated on an apple-tree family. *Agronomie* **19**: 163–184.

Harrington CA, DeBell DS. 1996. Above- and below-ground characteristics associated with wind toppling in a young *Populus* plantation. *Trees – Structure and Function* **11**: 109–118.

Henderson R, Ford ED, Renshaw E, Deans JD. 1983. Morphology of the structural root system of Sitka spruce 1. Analysis and quantitative description. *Forestry* **56**: 121–135.

Jolivet C, Arrouays D, Lévèque J, Andreux F, Chenu C. 2003. Organic carbon dynamics in soil particle-size separates of sandy spodosols when forest is cleared for maize cropping. *European Journal of Soil Science* **54**: 257–268.

Köstler JN, Brückner E, Bibelriether H. 1968. *Die Wurzeln der Waldbäume.* Hamburg, Germany: Verlag Paul Parey.

Mason EG. 1985. Causes of juvenile instability of *Pinus radiata* in New Zealand. *New Zealand Journal of Forest Science* **15**: 263–280.

McMinn RG. 1963. Characteristics of Douglas-fir root systems. *Canadian Journal of Botany* **41**: 105–122.

Nicoll BC, Coutts MP. 1998. Timing of root dormancy and tolerance to root waterlogging in clonal Sitka spruce. *Trees – Structure and Function* **12**: 241–245.

Nicoll BC, Dunn AJ. 1999. The effects of wind speed and direction on radial growth of structural roots. In: Stokes A, ed. *Proceedings of the Conference 'The Supporting Roots of Trees and Woody Plants: Form, Function and Physiology', Bordeaux, 20–24 July 1998, Series: Developments in Plant and Soil Sciences,* Vol. 87. Dordrecht, the Netherlands: Kluwer Academic Publishers, 61–76.

Nicoll BC, Ray D. 1996. Adaptive growth of tree root systems in response to wind action and site conditions. *Tree Physiology* **16**: 891–898.

Nicoll BC, Easton EP, Milner AD, Walker C, Coutts MP. 1995. Wind stability factors in tree selection: distribution of biomass within root systems of Sitka spruce clones. In: Coutts MP, Grace J, eds. *Wind and trees.* Cambridge, UK: Cambridge University Press, 276–301.

O'Cinnéide MS. 1975. Aspect and wind direction as factors in forest stability: the case of Northern Ireland. *Journal of Biogeography* **2**: 137–140.

Oppelt AL, Kurth W, Dzierzon H, Jentschke G, Godbold DL. 2000. Structure and fractal dimensions of root systems of four co-occurring fruit tree species from Botswana. *Annals of Forest Science* **57**: 463–475.

Ray D, Nicoll BC. 1998. The effect of soil water-table depth on root-plate development and stability of Sitka spruce. *Forestry* **71**: 169–182.

Righi D, Wilbert J. 1984. Les sols sableux podzolisés des Landes de Gascogne (France): répartition et caractères principaux. *Science du Sol* **4**: 253–264.

Sinoquet H, Rivet P. 1997. Measurement and visualization of the architecture of an adult tree based on a three-dimensional digitising device. *Trees – Structure and Function* **11**: 265–270.

Sprent P. 1989. *Applied nonparametric statistical methods.* London, UK: Chapman & Hall.

Stokes A. 2002. Biomechanics of tree root anchorage. In: Weisel Y, Eshel A, Kafkafi U, eds. *Plant roots: the hidden half,* 3rd edn. New York, NY, USA: Marcel Dekker, 175–186.

Stokes A, Berthier S. 2000. Irregular heartwood formation in *Pinus pinaster* Ait. is related to eccentric, radial stem growth. *Forest Ecology and Management* **135**: 115–121.

Stokes A, Ball J, Fitter AH, Brain P, Coutts MP. 1996. An experimental investigation of the resistance of model root systems to uprooting. *Annals of Botany* **78**: 415–421.

Stokes A, Nicoll BC, Coutts MP, Fitter AH. 1997. Responses of young Sitka spruce clones to mechanical perturbation and nutrition: effects on biomass allocation, root development, and resistance to bending. *Canadian Journal of Forest Research* **27**: 1049–1057.

Tamasi E, Stokes A, Lasserre B, Danjon F, Berthier S, Fourcaud T, Chiatante D. 2005. Influence of wind loading on root system development and architecture in oak (*Quercus Robur* L.) seedlings. *Trees – Structure and Function* **19**: 374–384.

Watson A, O'Loughlin C. 1990. Structural root morphology and biomass of three age-classes of *Pinus radiata. New Zealand Journal of Forest Science* **20**: 97–110.

Wu HX, Yeh FC. 1997. Genetic effect on biomass partition and tree architecture in seedlings of *Pinus contorta* ssp. *latifolia* in Alberta, Canada. *Forest Genetics* **4**: 123–130.